JOURNAL OF OPTOELECTRONICS LASER ISSN:1005-0086

Volume 41 Issue 4, 2022

Archimedes Optimization Algorithm based Fractional MPPT for Enhancing Performance and Efficiency of Photovoltaic Systems

Hamid A. Abed Hannon*[1], Haider K. Latif[2] & Ahmad T. Abdulsadda[3]

[1,2]Al-Furat Al-Awsat Technical University, Technical College of Al-Mussaib, Babylon, Iraq

[3]Al-Furat Al-Awsat Technical University, Al Najaf Technical Engineering College, Najaf, Iraq

ABSTRACT This paper focuses on the solving the issues of maximum power point tracking (MPPT) for photovoltaic (PV) system. The main issues of conventional MPPT are slower response due to fixed step change, high ripple, higher oscillation due to swing about maximum power point (MPP). In order to solve these issues, the fractional optimizer MPPT is proposed in this paper. The novel metaheuristic algorithm, which is called Archimedes optimization algorithm (AOA), is proposed to tune the five parameters of Fractional Order Proportional Integral Derivative (FOPID) controller. The simulation results demonstrate the proposed MPPT is very effectiveness to reach the MPP under no uniform condition without overshoot and oscillation and very small ripple as compared with conventional MPPT and several intelligent strategies in literature papers. The efficiency of proposed MPPT is up to 99.53%.

Keywords: PV system, hybrid MPPT, AOA MPPT, Archimedes optimization algorithm, Luo DC-DC converter.

I. INTRODUCTION

Due to global warming, high fossil fuel costs, and the dangers they pose to the environment, the hunt for alternative sustainable green energy sources has captivated the world's attention. Solar energy is the most common renewable energy source. Solar energy is a non-polluting, long-lasting, and low-cost energy source. Photovoltaic (PV) (solar cell) systems are among the most beneficial systems, and their use is becoming more widespread. PV systems may be linked to the grid or operated independently [1, 2]. Solar irradiation, cell temperature, and load determine the quantity of electricity produced by a PV panel [3].

These significant recent global achievements have aroused academics in solar energy to address the domain's primary concerns: the energy conversion efficiency of photovoltaic (PV) systems. A PV system's efficiency is defined as the amount of electrical output produced per unit of incident irradiation. The most efficient Silicon (Si) crystalline cells and modules are 26.3 % and 24 %, respectively [4]. A control approach for obtaining Maximum Power Point (MPP) is used to extract maximum efficiency from the Si material's inherent limited efficiency. It plays a critical role in the functioning of a PV system [2,4,5].

Up to now, the total PV efficiency has been approximately 15%. To maintain the system running at maximum efficiency, maximum power point tracking (MPPT) is required. The MPP of the output power–voltage (P–V) curve may be tracked to increase the power provided by PV systems. Under partly darkened circumstances, this curve may have multi-local maximum points [4-7]. Compared to technologies that improve solar cell manufacture, using MPPT techniques is the most cost-effective way to improve the system's overall efficiency [8, 9].

The two most common forms of traditional Maximum Power Point Tracking (MPPT) approaches are incremental conductance (IC) and perturb and observe (P&O) [10-12]. These methods have been widely used because of their simplicity, ease of application, and cost-effectiveness. Each of these strategies, however, has its own set of disadvantages. P&O oscillates around MPP when a PV system achieves MPPT due to fluctuations in the operational point [1-3,13,14]. This is due to the employment of a fixed perturbation, which results in a loss of produced energy.

MPP is computed using approximation functions of open-circuit current and short circuit voltage in other basic techniques such as Fractional Open Voltage and Short Circuit procedures [7,10]. Because it considers fluctuations in current concerning voltage and helps with fast changes in irradiation, the IC MPPT method has a higher computational complexity than P&O. The uncertainty in selecting the step size and the ensuing oscillations, like with P&O, is a disadvantage of this approach [1-4]. Furthermore, P&O cannot follow MPP in quickly changing environmental circumstances.

PV systems are a problematic plant from the standpoint of control engineering because of their nonlinear properties. Variable climatic circumstances impact PV systems, necessitating the use of a simple and adaptable controller that can adjust to changing conditions [14]. As a result, a reliable and straightforward controller is required to track the

MPP in real-time and precisely under all operational situations. Traditional MPPT trackers fail to provide these adaptive and robust control criteria under changing environmental circumstances [7]. Artificial Neural Network (ANN) based methods [15], fuzzy logic [16], and metaheuristics like cuckoo search (CS), grey wolf optimizer (GWO), Particle Swarm Optimization (PSO) are presented in [14]. However, these technologies' computational complexity-based limitations restrict their practical application to traditional procedures.

Furthermore, ANN-based MPPT methods require a considerable quantity of data for appropriate training (various irradiations, temperatures, and partial shade situations), making them viable only for big PV panels [17]. Furthermore, while searching for the optimal value, metaheuristics-based techniques suffer from severe transient behaviour (duty cycle or reference voltage). Under rapidly shifting environmental circumstances, this results in delayed convergence and may even result in premature convergence [7]. Fuzzy Logic Control (FLC) has a medium computational complexity and is equivalent to ANN efficiency. However, FLC design necessitates a thorough understanding of PV functioning, and the FLC rule table, if not optimized appropriately, can result in additional computation.

Various combinations of clever approaches were investigated to counteract these disadvantages. The FLC's membership functions and rules were optimized using PSO [18]. [19] proposes an FLC combined with a Hopfield ANN to overcome FLC's static fuzzy rule table. Bat algorithm based MPPT [20]. Grey wolf optimizer based MPPT [21,22]. Machine learning-based MPPT [23].
For MPPT, artificial intelligence (AI) based technologies have been widely used and combined with other techniques. However, the practical implementation of complex MPPT systems is limited due to declining solar cell prices. Traditional MPPT techniques such as P&O, IC, and Proportional-Integral-Derivative (PID) must be improved by researchers [7].

This paper presents a new hybrid Archimedes optimization algorithm (AOA) with an IC algorithm to enhance the performance and efficiency of PV systems under non-uniform conditions. The primary goal of this study is to create efficient MPPT hybrid algorithms that solve the limitations that traditional approaches have when dealing with abrupt changes and partial shading. The suggested approach is a blend of the AOA and the IC algorithms. Another goal is to evaluate the performance of two hybrid algorithms developed by FLC and P&O [36] with the existing hybrid algorithm under various weather situations. AOA quickly takes the system close to the MPP and enables smaller step sizes in the P&O and IC algorithms, resulting in improved accuracy and reduced oscillations. Building MATLAB/Simulink models of the PV system, super lift Luo converter, and controllers are used to examine the performance of the suggested techniques. To evaluate the performance of the proposed hybrid algorithm, it is compared to standalone FLC, IC, and P&O controllers.

II. PROPOSED SYSTEM

The proposed configuration is composed of three units which are PV modules, super Lift Luo DC/DC converters, and fractional optimizer MPPT algorithm, as depicted in figure (1). The PV system consists of a three-string, and each string includes three panels, as shown in figure (1). The total output power of the PV system is approximately (2340 W), and each PV module has 260 W, which in turn includes 60 cells. The specification parameters of the PV module are listed in Table 1. The design, mathematical model and analysis of each unit of the proposed configuration is explained in sub-section, which are included an introduction to optimizer algorithm called Archimedes optimization algorithm (AOA) and how to employee it for fractional MPPT controller, which is employed in this study to deal with a wide range of non-uniform conditions. Finally, the whole design of the super Lift Luo DC/DC converter is presented.

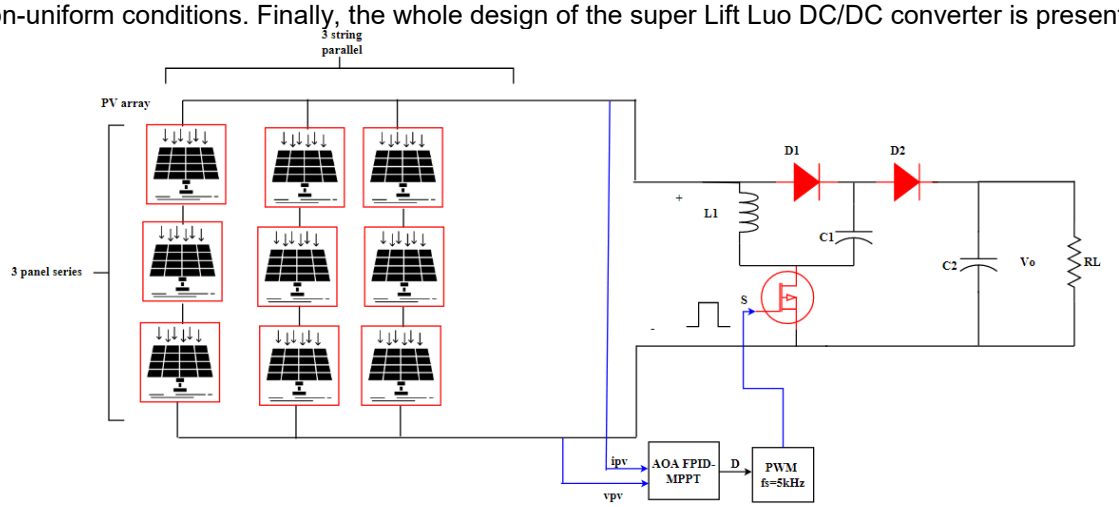

Figure 1. Proposed system configuration

Table 1. Specification parameters of BS-SP260/24Vtype

Name	Symbol	Value
Rated Power	P_{max}	260 W
Open Circuit Voltage	V_{oc}	37.6 V
Rated Voltage	V_{mpp}	31 V
Short Circuit Current	I_{sc}	8.88 A
Rated Current	I_{mpp}	8.4 A
Normal operation condition temperature	NOCT	45° C+/-2° C
Maximum System Voltage	V_L	1000 V
Series Fuse Rating	SFR	15 A

Mathematical Model PV Cell

Because it excludes the influence of series and parallel resistance, the ideal photovoltaic cell model depicted in Figure 1(a) is the simplest PV model. The I–V characteristics of a cell describe its output current, which is stated mathematically as [24]:

$$I_{PV} = I_{Ph} - I_d \quad (1)$$

To acquire exact results, a series resistance (R_S) is usually added to the perfect cell model. This model, despite its simplicity, displays inadequacies when exposed to temperature fluctuations. This model has been enhanced by the addition of a shunt resistance (R_{sh}). As illustrated in Figure 1(b), this single diode or five parameter model consists of a current producer and a diode with series and shunt resistances. The series resistance indicates the resistance (ohmic loss) to current flow caused by ohmic contact (metal-semiconductor contact) and resistance caused by impurity concentrations and junction depth. Shunt resistance, R_{sh}It is connected parallel to the diode and represents leakage current across the junction. In Eq. (1), the mathematical expression of the output current is modified as follows:

$$I_{PV} = I_{Ph} - I_d - \frac{V_d}{R_{sh}} \quad (2)$$

where V_d is the diode voltage, denoted as:

$$V_d = V_{PV} + I_{PV}R_S \quad (3)$$

It is well established that series and shunt resistance affect the I–V characteristic curve of a photovoltaic device, which affects the output voltage. That shunt resistance reduces the available current. Eq. (4) described the single diode model of the PV cell is as follows:

$$I_{PV} = I_{Ph} - I_s\left[e^{\left(\frac{qV_d}{n\ KT}\right)} - 1\right] - \left[\frac{V_{PV}+I_{PV}R_S}{R_{sh}}\right] \quad (4)$$

The temperature and insolation dependence of the saturation current (I_s) and photogenerated current (I_{Ph}) in a photovoltaic cell. A solar photovoltaic cell's saturation current fluctuates as a cubic function of temperature, which is expressed by the following equation:

$$I_s = I_{rs}\left(T/T_r\right)^3 - e^{\left[\frac{q+E_{bg}}{nK}\left[\frac{1}{T_r}-\frac{1}{T}\right]\right]} \quad (5)$$

Reverse saturation current, ambient temperature, and energy band gap (1.1 eV) are represented by I_{rs}, T_r, and E_{bg}, respectively.

The following equation can be used to calculate the reverse saturation current at a temperature T:

$$I_{sr} = I_{sc}\Big/\left(e^{\left(\frac{qV_{oc}}{n\ KT}\right)} - 1\right) \quad (6)$$

Short circuit current and open-circuit voltage are represented by I_{sc} and V_{oc}, respectively. The saturation current is determined by the cell's current density and functional area. The intrinsic characteristic determines current density.

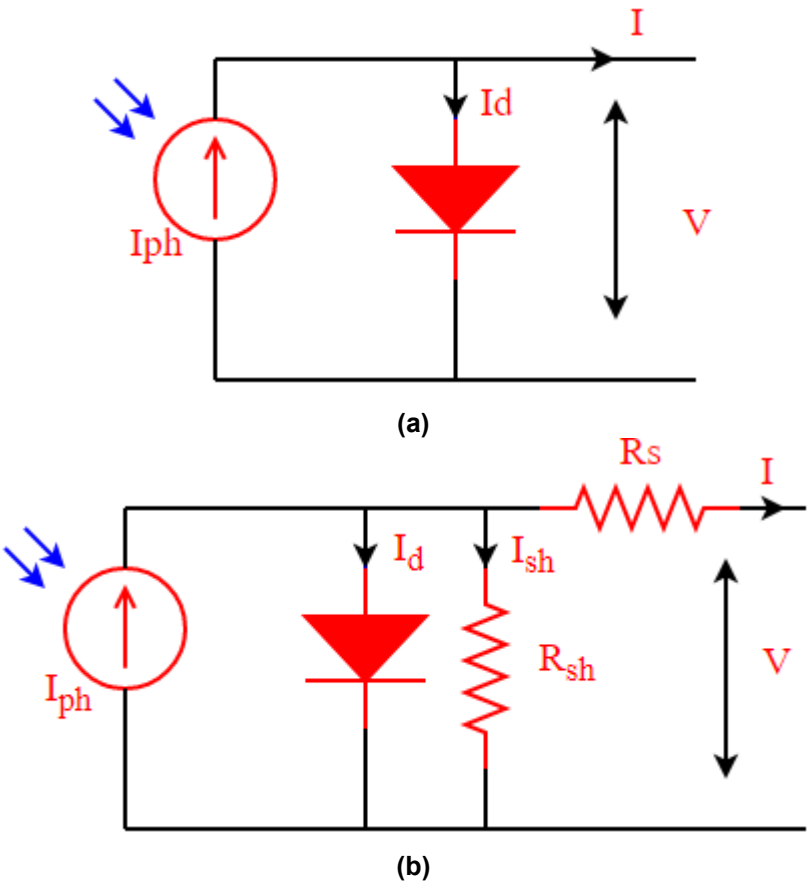

Figure 2.PV cell, (a) electrical ideal circuit, (b) electrical single diode circuit.

The above description is for a PV cell; depending on the application, the cells may be joined in series to provide high voltage or in parallel to increase current to build a PV module. Equations (2-6) [24] offer the usual mathematical formulation for resultant current for a double diode-based PV module when a PV cell model is scaled by adding strings of cells in parallel and cells in series. The mathematical modelling of double diode models is presented in the next paragraph to anticipate solar photovoltaic cells' electrical properties accurately.

Super Lift Luo DC-DC converter

One of the main elements that contribute to investigating the maximum power under shading conditions is the DC-DC converter. The basic step-up converter is called boost converter, which has some merits such as simple structure and operation and simple implementation. However, it has drawbacks like low gain ratio, reverse recovery diode under the higher value of duty cycle (D>0.7) and high voltage stress on active switch [25]. This paper uses the super positive Luo converter rather than a simple boost converter. The Luo Converter is a DC-DC converter that works similarly to a boost converter. Compared to a boost converter, the Luo Converter has a higher gain ratio, lower output ripple of voltage and current, and assisted the MPPT algorithm in reaching maximum power as quickly.

The basic concept of a super positive Luo converter depends on charging the passive elements in parallel during ON mode and discharge in series during off mode, as shown in figure (3 (b and c)). From this principle, the gain ratio can be written as [26-28]:

$$\frac{V_o}{V_{in}} = \frac{2-D}{1-D} \quad (7)$$

When ignoring the losses, the input current can be found out as,

$$I_{in} = \frac{2-D}{1-D} I_o \quad (8)$$

The design of passive elements is essential to operate the DC-DC converter perfectly with the MPPT algorithm. The output capacitor is driven based on the variation ripple in output voltage and can be expressed as:

$$C_2 = \frac{1-D}{2\,R\,f_S\,\Delta V_{C2}} \quad (9)$$

The pumping inductor can be designed during ON mode as,

$$L_1 = \frac{D\,V_{in}}{f_S\,\Delta I_{L1}} \quad (10)$$

Finally, the lift capacitor can be designed depending on the relationship between voltage and current of principle operation capacitor and the working principle of super positive Luo converter as:

$$C1 = \frac{I_{in}(1-D)}{(2-D)\, f_S \Delta V_{C1}} \quad (11)$$

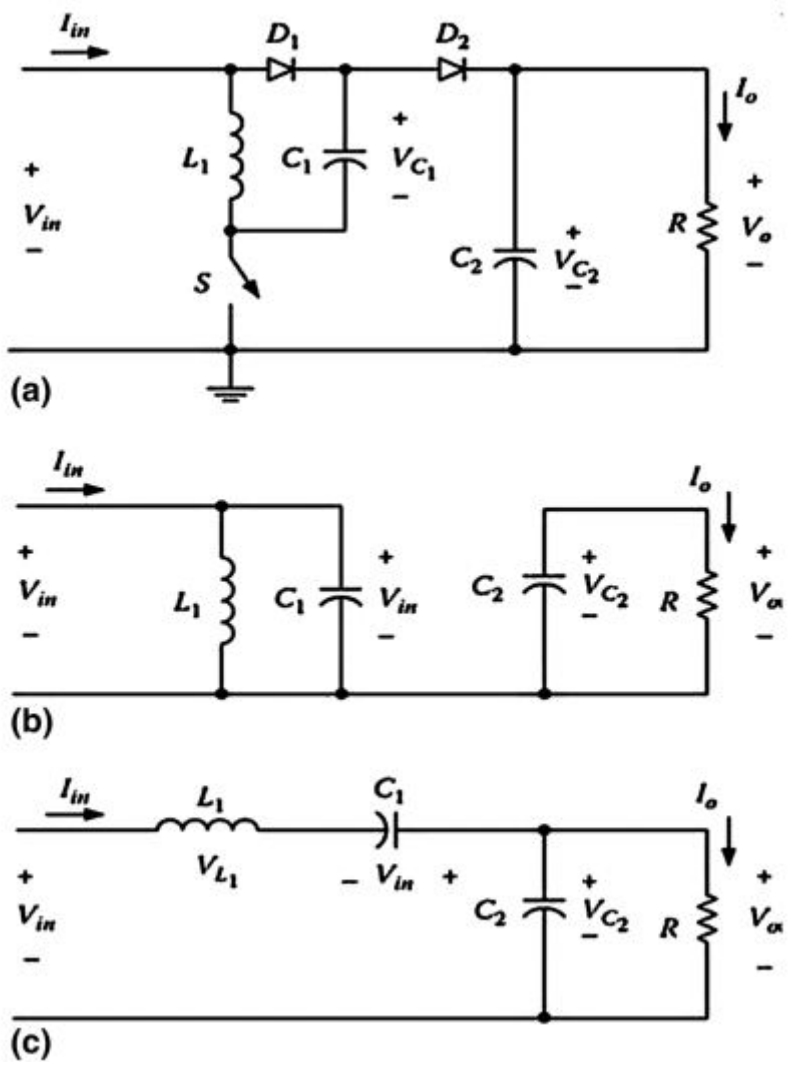

Figure 3.equivalent circuit of positive super lift Luo converter, (a) elementary circuit (b) ON switch, (c) off switch

III. ARCHIMEDES OPTIMIZATION ALGORITHM (AOA)

The AOA algorithm is dependent on the population. Individuals in the population are immersing objects in the suggested method. Like other population-based metaheuristic algorithms, AOA begins the search process by populating a set of objects (candidate solutions) with random volumes, densities, and accelerations [29]. Each item is also given a random position in fluid at this point. AOA operates in iterations until the termination condition is met after assessing the fitness of the original population. AOA adjusts the density and volume of each item in each loop. The item's acceleration is modified depending on the situation of its collision with any other nearby object. The new position of an item is determined by its updated density, volume, and acceleration.

The detailed mathematical formulation of AOA stages is shown below according to [29].

Initialization

The position initializing of all objects can be expressed as:

$$O_i = lb_i + rand \times (ub_i - lb_i); i = 1.2. \ldots . N \quad (12)$$

In a population of N objects, O_i is the i[th] object. The bottom and upper boundaries of the search space are denoted by $ub_i \; and \; lb_i$, respectively.

In order to start the search randomly, the volume (vol) and density (den) for each i[th] object are depicted in equation (13):

$$den_i = rand$$
$$vol_i = rand \quad (13)$$

where $rand$is a D-dimensional vector that produces a number between 0 and 1 at random. Finally, using (14), initialize the acceleration (acc) of the i[th]object:

$$acc_i = lb_i + rand \times (ub_i - lb_i) \quad (14)$$

Evaluate the original population and choose the item with the best fitness value in this stage. Assign the x_{best}, den_{best}, vol_{best}, and acc_{best} to the next step.

Update densities, volumes

After that, equation (15) is used to update the density and volume of an item i for iteration $t+1$:

$$den_i^{t+1} = den_i^t + rand \times \left(den_{best} - den_i^t\right)$$
$$vol_i^{t+1} = vol_i^t + rand \times \left(vol_{best} - vol_i^t\right) \quad (15)$$

where $vol_{best}$and den_{best} Denote the volume and density of the best item discovered thus far, and $rand$ denotes a uniformly distributed random integer.

Transfer operator and density factor

Initially, items collide, and after some time, the objects attempt to establish a condition of equilibrium. This is accomplished in AOA via the transfer operator T F, which converts search from exploration to exploitation, as specified by (16):

$$TF = exp\left(\frac{t-t_{max}}{t_{max}}\right) \quad (16)$$

where T F is steadily increased over time until it reaches 1. Iteration number t and maximum iterations t_{max} Similarly, the density-decreasing factor d aids AOA when searching globally to a local level. As specified by (17), it becomes smaller over time: are the iteration number and maximum iterations, respectively.

$$d^{t+1} = exp\left(\frac{t_{max}-t}{t_{max}}\right) - \left(\frac{t}{t_{max}}\right) \quad (17)$$

where d^{t+1} decreases over time, allowing convergence in a previously selected suitable region. It's worth noting that careful control of this variable will guarantee that exploration and exploitation in AOA are balanced.

Exploration phase

If T F ≤ 0.5, objects collide, choose a random material (mr) and change the object's acceleration for iteration t + 1 using (18):

$$acc_i^{t+1} = \frac{den_{mr}+vol_{mr}\times acc_{mr}}{den^{t+1}{}_i \times vol^{t+1}{}_i} \quad (18)$$

Density, volume, and acceleration of item i are represented by $den_i, vol_i \; and \; acc_i$. The acceleration, density, and volume of random material are represented by $acc_{mr}, den_{mr}, and \; vol_{mr}$, respectively. It's worth noting that T F ≤ 0.5 guarantees exploration for one-third of iterations. When a number other than 0.5 is used, the behaviour of exploration and exploitation is altered.

Exploitation phase

If there is no collision between objects and TF > 0.5, change the acceleration of the object for iteration t + 1 using (19):

$$acc_i^{t+1} = \frac{den_{best}+vol_{best}\times acc_{best}}{den^{t+1}{}_i \times vol^{t+1}{}_i} \quad (19)$$

where acc_{best} is the best object's acceleration.

Normalize acceleration

To get the percentage of change, normalize the acceleration can be calculated using (20):

$$acc_{i-norm}{}^{t+1} = u \times \frac{acc_i^{t+1} - min(acc)}{max(acc) - min(acc)} + l \quad (20)$$

The normalization ranges u and l are set to 0.9 and 0.1, respectively. The acc_{i-norm} Specify the percentage of each agent's step that will change. If item I is distant from the global optimum, its acceleration value is high, indicating that it is in the exploration phase; otherwise, it is in the exploitation phase. This diagram shows how the search progresses from exploration to exploitation. In most cases, the acceleration factor starts high and then lowers over time. This assists search agents in moving towards the most outstanding global solution while also moving away from local ones. However, it is worth noting that a few search agents may require more time in the exploration phase than in the typical scenario. As a result, AOA achieves a good mix between exploration and exploitation.

Update position

If T F ≤ 0.5 (exploration phase), the position of the i[th] object for the next iteration t + 1 can be expressed as:

$$x_i{}^{t+1} = x^t{}_i + C_1 \times rand \times acc_{i-norm}{}^{t+1} \times d \times (x_{rand} - x_i{}^t) \quad (21)$$

where C_1 = 2 and C_2 = 1. Otherwise, if TF > 0.5 (exploitation phase), the objects use this method to update their positions by using equation (22).

$$x_i{}^{t+1} = x^t{}_{best} + F \times C_2 \times rand \times acc_{i-norm}{}^{t+1} \times d \times (T \times x_{best} - x_i{}^t) \quad (22)$$

C2 is a constant that equals 6. T is directly proportional to the transfer operator and is defined as $\mathrm{T} = \mathrm{C}_3 * \mathrm{T\,F.T}$ rises with time and is directly proportional to the transfer operator. T grows with time in the range [C3 ×0.3, 1] and initially subtracts a specific percentage from the best position. It begins with a low percentage because this results in a wide disparity between the best and current positions, causing the random walk's step size to be huge. As the search progresses, this percentage steadily rises, reducing the gap between the best and current positions. As a result, a suitable balance between exploration and exploitation may be achieved.

To change the direction of motion, use the F flag by equation (23).

$$F = \begin{cases} +1 \; if \; P \le 0.5 \\ -1 \; if \; P > 0.5 \end{cases} \quad (23)$$

Where $P = 2 \times rand - C_4$

Evaluation

Use the objective function f to evaluate each object and keep track of the best solution found so far. Assign x_{best}, den_{best} , vol_{best}, and acc_{best}.

IV. PROPOSED MPPT AND OBJECTIVE FUNCTION

The conventional MPPT has drawbacks such as slower response under partial shading conditions, higher ripple at a lower level of irradiation and higher oscillation due to swing about the MPP [5]. In addition, one of most issues of traditional MPPT depends on fixed step-change duty cycle ΔD which is caused the slower response due to assuming constant value and the next duty cycle can be increased or decreased by this value as depicted in equation (24). The proposed hybrid MPPT strategy suggests a duty cycle with each temperature variation, irradiation, and load to solve these issues. In this paper, the suggested MPPT depends on the principle of incremental conductance algorithm, which is $\frac{\mathrm{i_{pv}}}{\mathrm{v_{pv}}} + \frac{\mathrm{di_{pv}}}{\mathrm{dv_{pv}}} = 0$to investigate MPP. From this concept, the first step of the proposed MPPT is calculated condition by measuring the voltage and current of the PV system. After that, compared with zero, the condition of investigating the maximum power is demonstrated in Figure 4. The output error is input to the fractional-order PID (FOPID) controller to correct the system and harvest maximum power from the PV system. The hybrid AOA is employed to tune the FOPID controller for investigating the fast-tracking of maximum power under non-uniform conditions. The fitness used to tune the parameters of the FOPID controller is Integral Time Absolute Error (ITAE). The ITAE equation can be expressed by equation (25):

$$D_{i+1} = D_i \mp \Delta D \quad (24)$$

$$j_{min} = \int_0^t t \times \left(\left| 0 - \frac{\mathrm{i_{pv}}}{\mathrm{v_{pv}}} + \frac{\mathrm{di_{pv}}}{\mathrm{dv_{pv}}} \right| \right) dt \quad (25)$$

Where $j_{min} is\ the\ minimum\ fitness$, t is the simulation error.

The optimal parameters of FOPID based on AOA used in simulation results are presented in Table 2

Table 2. Optimal gain of PID and FOPID based AOA.

parameters		PID	FOPID
	Kp	7.847	8.1074
	Ki	0.15542	0.142
	Kd	0.0052	0.000131
λ		-	1.2
μ		-	0.0014
	j_{min}	4.355	0.345

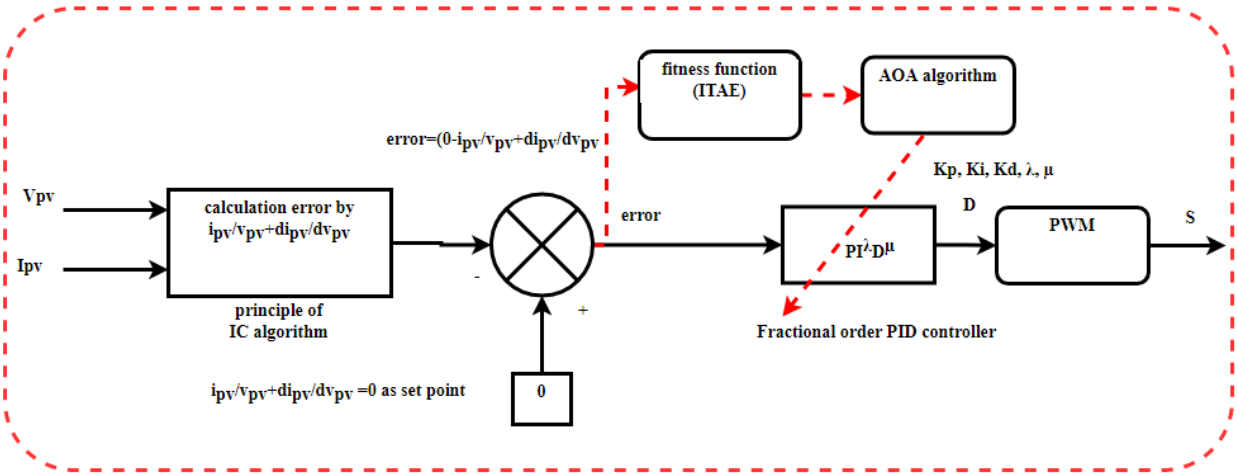

Figure 4.AOA-FOPID based on MPPT of PV systems.

V. PERFORMANCE INDICES

To assess the proposed MPPT based on the AOA algorithm, various indices are used to describe the behaviours of the proposed MPPT and compared with other algorithms during static and dynamic changes. The following are the indices that are used in this paper to evaluate the performance and efficiency of MPPT, according to [30]:

Accuracy $\boldsymbol{\alpha_{MPPT}}$: This index is used to determine how nearly the tracking is to reach its maximum point. It was utilized in our study to show how near the PV current is to the current maximum power point during tracking, as seen below:

$$\alpha_{MPPT} = \frac{I_{pv}}{I_{MPPT}}.100 \qquad (26)$$

Index of static efficiency $\boldsymbol{\eta_{MPPT}}$: The MPPT graph depicts the ratio of actual PV power to maximum PV power. It is provided by:

$$\eta_{MPPT} = \frac{P_{pv}}{P_{MPPT}}.100 \qquad (27)$$

Relative tracking error $\boldsymbol{\epsilon_{MPPT}}$: is expressed as follows:

$$\epsilon_{MPPT} = \left|\frac{P_{pv}}{P_{MPPT}} - 1\right|.100 \qquad (28)$$

In addition, the indices Eq. (29) and Eq. (30), which reflect MPPT energetic efficiency and MPPT energizing error, are used to compare the tracking performance of the proposed and standard methods during dynamic changes in the MPP.

$$\eta_{MPPT,E} = \left(\frac{\int_0^{t_f} P_{pv}\,dt}{\int_0^{t_f} P_{MPPT}\,dt}\right).100 \qquad (29)$$

$$\epsilon_{MPPT,E} = \left(\frac{\int_0^{t_f} P_{pv}\,dt}{\int_0^{t_f} P_{MPPT}\,dt} - 1\right).100 \qquad (30)$$

VI. RESULTS AND DISCUSSION CONCLUSION

The proposed system is tested under climate change to corroborate the model and make the simulation results more realistic. In this work, the BS-SP20/24Vtype is employed. Table I lists the most critical parameters for this type in Matlab/Simulink. The parameter of PID tuned by AOA-PID and AOA are listed in table II.

While a controller's MPPT tracking efficiency may be excellent under static settings, it can drop dramatically under quickly changing environmental conditions, especially with irradiation. As a result, performance evaluation in the face of constantly changing environmental conditions is critical. This part addresses rapidly changing environmental circumstances, which are very frequent daily. The irradiance changes fast while the temperature is kept constant in this test instance and vice versa.

Irradiation Variation

Figure 5 depicts the profile that was utilized for this test scenario. It should be observed that this fluctuation occurs between a low irradiation level of 500 and the most excellent irradiation level conceivable, 1000. Furthermore, the temperature is maintained as STC (25C) during the irradiation fluctuation The resulting MPPT responses for PV current, voltage and maximum power are shown in Figs. (6, 7, and 8), and the performance of hybrid AOA-PID and

cuckoo search algorithm MPPT controllers has superiority over the AOA-PID MPPT controller in terms of fast-tracking to the maximum power despite quickly variable irradiation with the minimal period.

Figures 6 and 7 indicate the proposed PV current and voltage controller. It can be seen from these figures, the proposed MPPT based on AOA has a lower ripple and maximum undershoot than the AOA-PID-based MPPT controllers. It's worth noting that this increase in power is caused by a shift from a low-irradiation zone to a higher-irradiation zone after a short period. Most traditional and intelligent MPPT controllers, as previously stated, fail to track success in these situations. The proposed MPPT controller, on the other hand, does not lose track and prevents the system response from deviating from the set-point.

Finally, the P-V curve of the irradiation test is depicted in figure 9. It can be noted from this figure when compared to existing MPPTs, and the proposed MPPT achieves the least amount of ripple and fast-tracking to the desired point without oscillation.

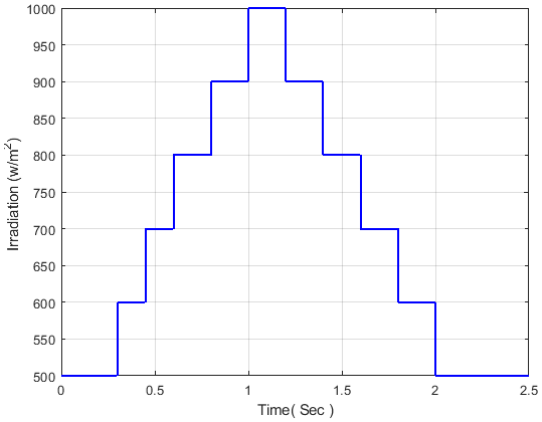

Figure 5. non-uniform irradiance

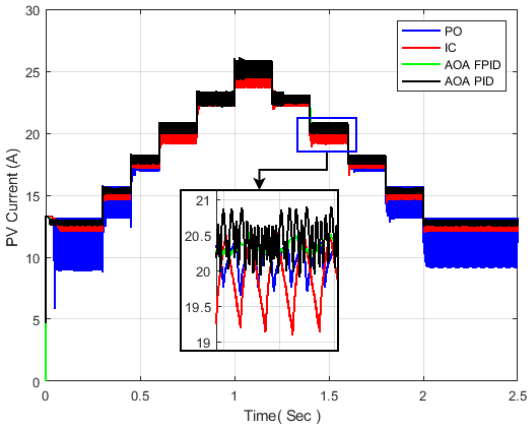

Figure 6.PV current response under non-uniform irradiance

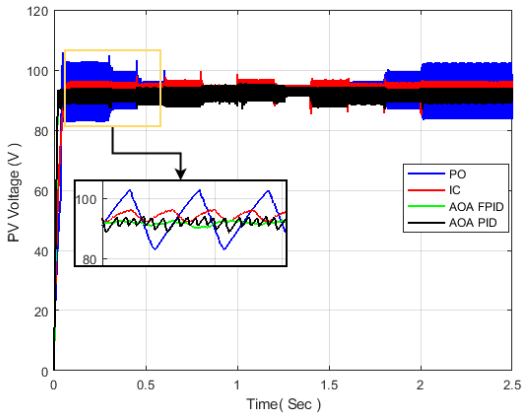

Figure 7. PV voltage response under non-uniform irradiance

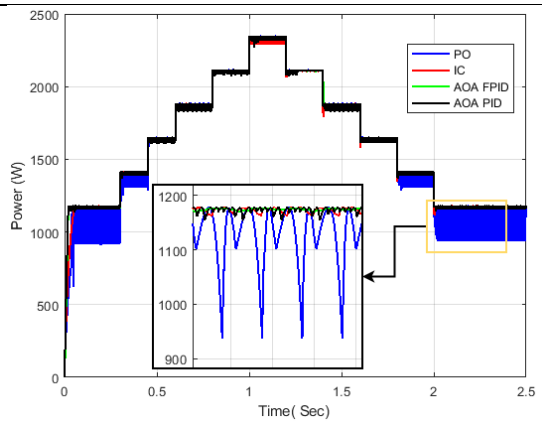

Figure 8.PV power of proposed system under non-uniform irradiance

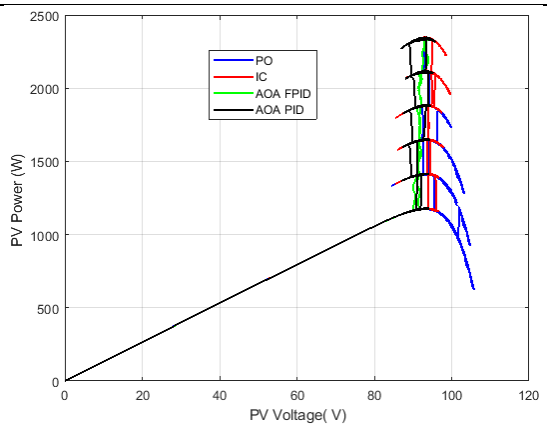

Figure 9.P-V curve under irradiation variation

Temperature Variation

Figure 10 depicts the profile that was utilized for this test scenario. It should be emphasized that this fluctuation occurs between medium temperature levels, such as 40, and the maximum temperature, such as 75 C. Irradiation was also kept constant during these temperature changes, as it was at STC.

Figure 11 shows the MPPT responses that were received. Compared to irradiation fluctuations, temperature variations do not generate significant changes in performance. However, performances at three locations have been examined in-depth and are shown here. As can be shown in Figs. 11, 12 and 13, the proposed hybrid AOA controller has less undershot than the AOA-PID based MPPT controllers. The comparative performance of controllers for maximum power is shown in figure (13). The performance gains are not as dramatic as the irradiation day profile, as can be observed. It can be seen from this figure, the proposed MPPT based on AOA still provides a minimum of energy loss with zero oscillation and a tiny ripple. This confirms the advantage of hybrid AOA-PID with cuckoo search based MPPT controllers for achieving MPPT during daytime heat conditions.

Figure 14 show the MPPT responses obtained in terms of the P-V curve. It can be seen from this figure, the proposed MPPT based on AOA-FOPID still provides a minimum of energy loss with zero oscillation and minimal ripple. This confirms the advantage of hybrid AOA-FOPID based MPPT controllers for achieving MPPT during daytime temperature.

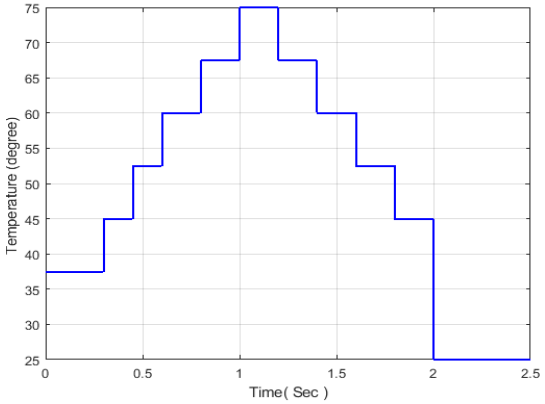

Figure 10.Change profile of temperature

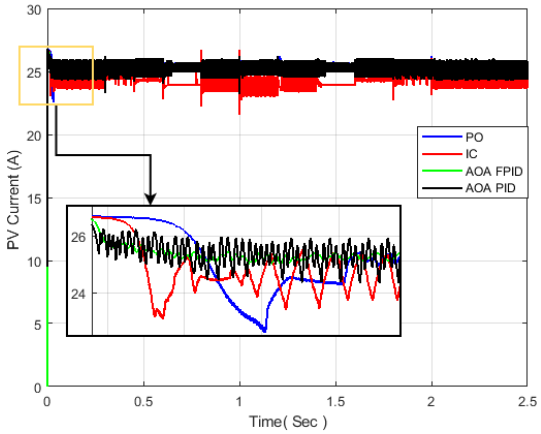

Figure 11.Dynamic response of PV current under variable temperature

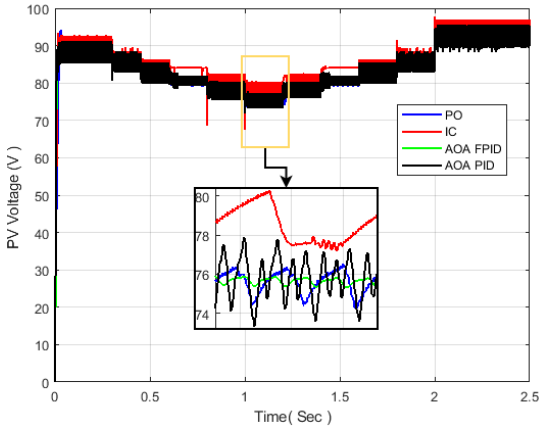

Figure 12. Dynamic response of PV voltage under variable temperature

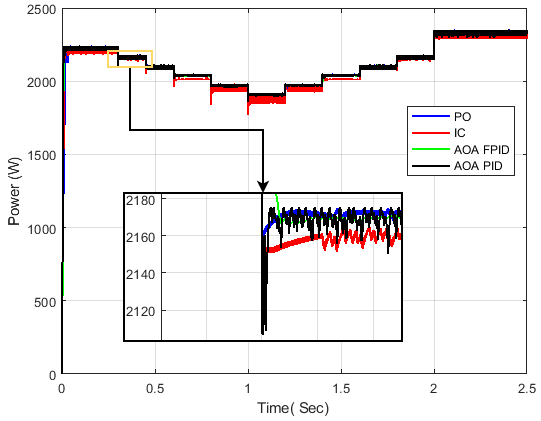

Figure 13.Dynamic response of PV power under variable temperature

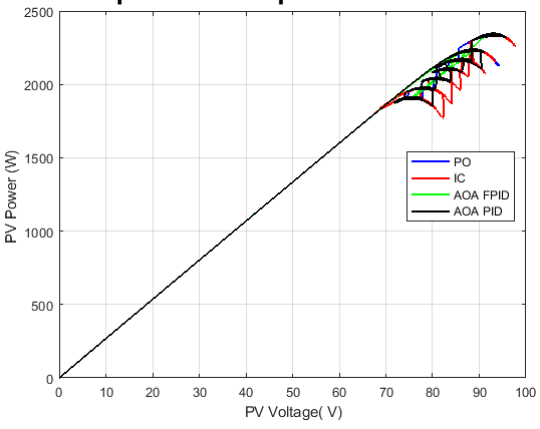

Figure 14.P-V curve under temperature variation

Simultaneous variations of temperature and irradiation

A final characteristic test is a combination of irradiance and temperature variations. The profile utilized is shown in Figures 15 and 16. As seen in Figs. 15 and 16 include both sharp and smooth fluctuations in irradiation and temperature. It acts as a chaotic and sudden profile under which the PV system may be required to operate.

Figures 17-19 illustrate the MPPT responses for combined temperature and irradiation changes. Figures 15 and 16 show that, compared to other MPPT controllers, the MPPT-based hybrid AOA controller has a minor degree of undershoot and the fastest tracking to temperature and irradiance changes that occur randomly. AOA-based MPPT, on the other hand, recovers faster than AOA-PID-based MPPT. When both controllers are approaching the point where the power to the left and right are nonlinear in relation, the AOA-PID MPPT stops tracking direction, causing significant undershoot at 0.3S and 0.5S. Still, the AOA based MPPT controller tracks the intended power with no variation. AOA-based MPPT controllers, as previously indicated, can recover more quickly from changes in direction in tracking intended power. The hybrid optimizer controller had the quickest settling time because other controllers still created significant oscillatory activity after achieving MPPT. Finally,as shown in Figs. 17-19, compared to the AOA-PID based MPPT, it is evident that the AOA based MPPT controller creates a minor ripple at steady-state under non-uniform conditions.

Finally, to prove the AOA-FOPID is reached maximum power tracking without oscillation and with a higher steady-state, the P-V curve is demonstrated in figure 20. It can be seen from this figure that the AOA-FOPID is reached the maximum point without swinging about the maximum point as compared with conventional P&O and AOA-PID strategies.

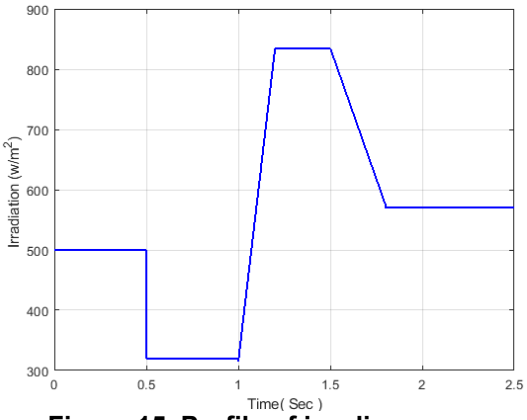

Figure 15. Profile of irradiance

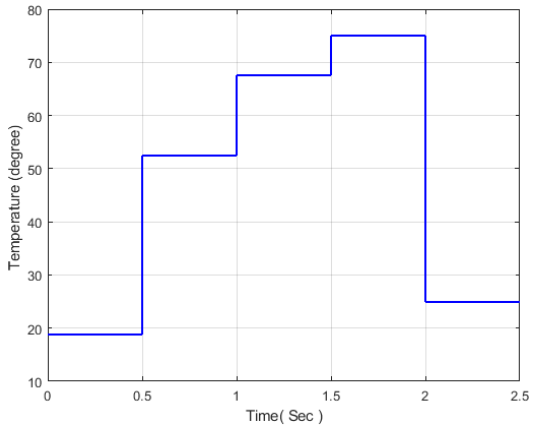

Figure 16.Profile of variable temperature

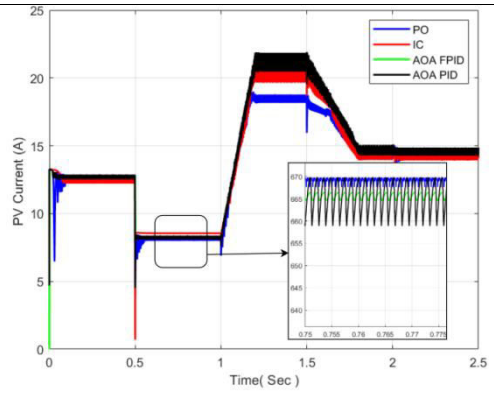

Figure 17.Dynamic response of PV current under variable temperature and irradiance

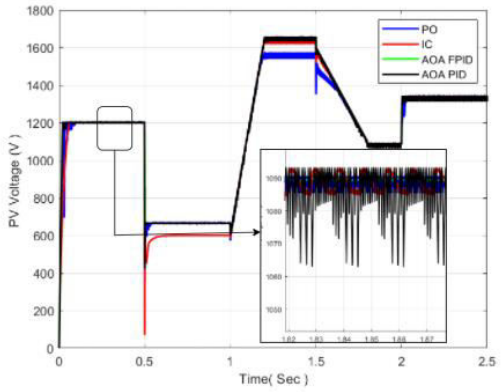

Figure 18.Dynamic response of PV voltage under variable temperature and irradiance

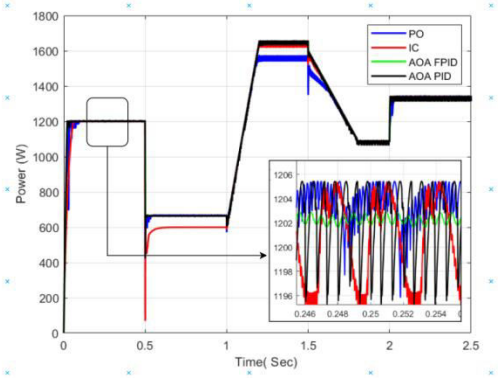

Figure 19. Dynamic response of PV power under variable temperature and irradiance

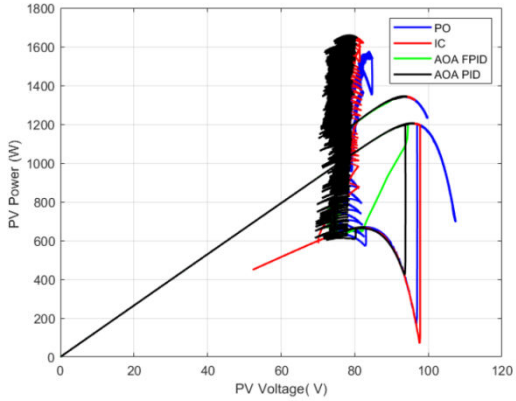

Figure 20.P-V curve under variation irradiation and temperature

VII. COMPARISONS PERFORMANCE AMONG THE MPPT STRATEGIES

As can be seen from the previous findings, the proposed AOA-based FOPID algorithm has a faster tracking speed and provides better efficiency and power quality than the conventional one.

Tables 3 and 4 show the values of the considered indices for the proposed and standard MPPT algorithms under variable irradiation and temperature conditions for the power response. The proposed AOA-based FOPID MPPT algorithm produces better performance in all regions of the system responses than the AOA-based PID MPPT and conventional P&O and IC algorithms. In this regard, as shown in the tables, the AOA-based PID MPPT outperformed the P&O and IC algorithms.

Table 3. Performances comparisons of proposed MPPT with conventional MPPT algorithms under variation irradiation.

Performance Index	P&O MPPT	IC MPPT	AOA-PID MPPT	AOA-FOPID MPPT
α_{MPPT}	94.34	95.61	98.847	99.44
η_{MPPT}	94.012	95.301	98.7545	99.5303
ϵ_{MPPT}	5.42	4.73	2.645	1.124
$\eta_{MPPT,\ E}$	94.501	95.63	98.92	99.552
$\epsilon_{MPPT,\ E}$	5.57	4.89	2.7021	1.2602

Table 4. Specification performances under variation irradiation.

Index	P&O MPPT	IC MPPT	AOA-PID MPPT	AOA-FOPID MPPT
Rise time (ms)	10.124	9.714	4.12	3.408
Settling time(ms)	13. 5	10.042	6.45	4.84
Overshoot (watt)	47.5	23.145	7.1445	0.4102
undershoot(watt)	85.47	38.145	9.45	0.452
Ripple(watt)	400.2	150.42	18	1.45

VIII. CONCLUSION

This study presents a modified MPPT based on a novel optimizer fractional PID and the principle of incremental conductance (IC) algorithm to reach fast seeking about MPP under various critical conditions. The proposed optimizer used to tune the five parameters is called AOA. The main advantages of the proposed MPPT are straightforward implementation, higher efficiency, and dealing with a wide range of issues of conventional MPPT. The simulation results show the suggested algorithm has outstanding performance compared with conventional MPPT and several intelligent algorithms in terms of high-speed tracking of MPP, no overshoot and oscillation, and higher efficiency reach to 99.53%.AOA-based fractional MPPT has a zero failure rate, a convergence time of less than 0.034 s, and zero oscillations around the steady-state conditions for any partial shade circumstances.

REFERENCES

[1] K. Bataineh, ‘‘Improved hybrid algorithms-based MPPT algorithm for PV system operating under severe weather conditions,’’ IET Power Electron., vol. 12, no. 4, pp. 703–711, Apr. 2019

[2] N. A. Kamarzaman and C. W. Tan, "A comprehensive review of maximum power point tracking algorithms for photovoltaic systems," Renewable & Sustainable Energy Reviews, vol. 37, pp. 585-598, Sep 2014.

[3] A. Ali *et al*., "Investigation of MPPT Techniques Under Uniform and Non-Uniform Solar Irradiation Condition–A Retrospection," in *IEEE Access*, vol. 8, pp. 127368-127392, 2020.

[4] Verma, Preeti, et al. "Meta-Heuristic Optimization Techniques Used for Maximum Power Point Tracking in Solar PV System," Electronics vol.10, no.19 pp. 2419, 2021.

[5] Sarvi, Mohammad, and Ahmad Azadian. "A comprehensive review and classified comparison of mppt algorithms in pv systems," Energy Systems,pp.1-40, 2021.

[6] L. Xu, R. Cheng, and J. Yang, ‘‘A new MPPT technique for fast and efficient tracking under fast varying solar irradiation and load resistance,’’ Int. J. Photoenergy, vol. 2020, pp. 1–18, Feb. 2020.

[7] D. Kler, K. P. S. Rana, and V. Kumar, “A nonlinear PID controller based novel maximum power point tracker for PV systems,” Journal of the Franklin Institute, vol. 335, no. 16, pp. 7827-7864, Nov. 2018.

[8] Nadeem, Ahsan, and AfaqHussain. "A comprehensive review of global maximum power point tracking algorithms for photovoltaic systems," *Energy Systems*, pp.1-42, 2021..

[9] Aldosary, Abdallah, et al. "A modified shuffled frog algorithm to improve MPPT controller in PV System with storage batteries under variable atmospheric conditions." *Control Engineering Practice* vol.1, no. 12, pp.104831, 2021.

[10] Eltamaly, Ali M. "A novel musical chairs algorithm applied for MPPT of PV systems." *Renewable and Sustainable Energy Reviews* 146 (2021): 111135.

[11] Eltamaly, Ali M. "An Improved Cuckoo Search Algorithm for Maximum Power Point Tracking of Photovoltaic Systems under Partial Shading Conditions." *Energies* 14.4 (2021): 953.
[12] Guo, Ke, et al. "An improved gray wolf optimizer MPPT algorithm for PV system with BFBIC converter under partial shading." *Ieee Access* 8 (2020): 103476-103490.
[13] Rezk, Hegazy, MokhtarAly, and Ahmed Fathy. "A Novel Strategy Based on Recent Equilibrium Optimizer to Enhance the Performance of PEM Fuel Cell System through Optimized Fuzzy Logic MPPT." *Energy* (2021): 121267.
[14] Rezk, Hegazy, et al. "A novel statistical performance evaluation of most modern optimization-based global MPPT techniques for partially shaded PV system." *Renewable and Sustainable Energy Reviews* 115 (2019): 109372.
[15] Messalti, Sabir, AbdelghaniHarrag, and AbdelhamidLoukriz. "A new variable step-size neural networks MPPT controller: Review, simulation and hardware implementation." *Renewable and Sustainable Energy Reviews* 68 (2017): 221-233.
[16] Ali, Mahmoud N., et al. "An efficient fuzzy-logic based variable-step incremental conductance MPPT method for grid-connected PV systems." *Ieee Access* 9 (2021): 26420-26430.
[17] Mohammadinodoushan, Mohammad, et al. "A new MPPT design using variable step size perturb and observe method for PV system under partially shaded conditions by modified shuffled frog leaping algorithm-SMC controller." *Sustainable Energy Technologies and Assessments* 45 (2021): 101056.
[18] Soufi, Youcef, MohceneBechouat, and Sami Kahla. "Fuzzy-PSO controller design for maximum power point tracking in photovoltaic system." *International Journal of hydrogen energy* 42.13 (2017): 8680-8688.
[19] Subiyanto, Subiyanto, Azah Mohamed, and M. A. Hannan. "Intelligent maximum power point tracking for PV system using Hopfield neural network optimized fuzzy logic controller." *Energy and Buildings* 51 (2012): 29-38.
[20] Kaced, Karim, et al. "Bat algorithm based maximum power point tracking for photovoltaic system under partial shading conditions." *Solar Energy* 158 (2017): 490-503.
[21] Mohanty, Satyajit, BidyadharSubudhi, and Pravat Kumar Ray. "A new MPPT design using grey wolf optimization technique for photovoltaic system under partial shading conditions." *IEEE Transactions on Sustainable Energy* 7.1 (2015): 181-188.
[22] Sharma, Satyam, RidhiKapoor, and SanjeevDhiman. "A Novel Hybrid Metaheuristic Based on Augmented Grey Wolf Optimizer and Cuckoo Search for Global Optimization." *2021 2nd International Conference on Secure Cyber Computing and Communications (ICSCCC)*. IEEE, 2021.
[23] Khan, NomanMujeeb, Umer Amir Khan, and Muhammad Hamza Zafar. "Maximum Power Point Tracking of PV System under Uniform Irradiance and Partial Shading Conditions using Machine Learning Algorithm Trained by Sailfish Optimizer." *2021 4th International Conference on Energy Conservation and Efficiency (ICECE)*. IEEE, 2021.
[24] Bana, Sangram, and R. P. Saini. "A mathematical modeling framework to evaluate the performance of single diode and double diode-based SPV systems." *Energy Reports* 2 (2016): 171-187.
[25] El-Ghanam, S. M. "Design, implementation and performance analysis of positive super-lift Luo-converter based on different MOSFET types." *Indian Journal of Physics* 94.6 (2020): 833-839.
[26] Dheeban, S. S., NB MuthuSelvan, and L. Krishnaveni. "Performance improvement of Photovoltaic panels by Super-Lift Luo converter in standalone application." *Materials Today: Proceedings* 37 (2021): 1163-1171.
[27] Luo, Fang Lin, and Hong Ye. "Positive output super-lift converters." *IEEE Transactions on Power Electronics* 18.1 (2003): 105-113.
[28] Shan, Zeng-li, Shuo Liu, and Fang-lin Luo. "Investigation of a Super-Lift Luo-Converter used in solar panel system." *2012 China International Conference on Electricity Distribution*. IEEE, 2012.
[29] Hashim, Fatma A., et al. "Archimedes optimization algorithm: a new metaheuristic algorithm for solving optimization problems." *Applied Intelligence* 51.3 (2021): 1531-1551.
[30] Ounnas, Djamel, et al. "Design and Hardware Implementation of Modified Incremental Conductance Algorithm for Photovoltaic System." *Advances in Electrical and Electronic Engineering* 19.2 (2021): 100-111.